Article:
Ma, Y, Ge, S, Yang, H orcid.org/0000-0003-4931-0168 et al. (1 more author) (2022) Coupled thermo-hydro-mechanical-chemical processes with reactive dissolution by non-equilibrium thermodynamics. Journal of the Mechanics and Physics of Solids, 169. 105065. ISSN 0022-5096

https://doi.org/10.1016/j.jmps.2022.105065

Coupled Thermo-Hydro-Mechanical-Chemical processes with reactive dissolution by non-equilibrium thermodynamics

Yue MA[1]*, Shangqi GE[1,2], He YANG[1], Xiaohui CHEN[1]

[1]School of Civil Engineering, University of Leeds, LS2 9JT, UK

[2]College of Civil Engineering and Architecture, Zhejiang University, Hangzhou, 310058, China.

[1]* Correspondence to: Yue MA, School of Civil Engineering, University of Leeds, LS2 9JT, UK
E-mail: cnym@leeds.ac.uk

Abstract

The Clausius-Duhem Inequality has been widely adopted to model the coupled Thermo-Hydro-Mechanical-Chemical processes. However, this paper points out that when modelling a reacting system, the Clausius-Duhem Inequality may hide the reaction mechanism and reaction type if the reaction changes the solid, and it may generate imprecise constitutive result if the reaction occurs within the fluid without changing the solid. To overcome these challenges, this paper proposed a novel non-equilibrium thermodynamics approach to model the multiphysics coupling processes with reactive dissolution. The new approach focuses on the Helmholtz free energy change in a dissolution process by quantifying the entropy production with the knowledge from non-equilibrium thermodynamics. A new concept, solid affinity, is introduced to give a better description of Helmholtz free energy change due to reactive dissolution. The coupled Thermo-Hydro-Mechanical-Chemical equations with reactive dissolution are derived by this approach. A numerical simulation is presented to show the role of quartz dissolution.

Keywords: THMC; Dissolution; Non-equilibrium thermodynamics; Clausius-Duhem Inequality

1 Introduction

Many geological settings, e.g., carbon capture and storage, nuclear waste disposal, geothermal system, are subject to coupled Thermo-Hydro-Mechanical-Chemical (THMC) process (Kolditz et al., 2016). Among these fours processes, the chemical process, especially reactive dissolution, often leads to significant changes of the physical and mechanical properties of the soil or rock. Through dissolution, the solid mineral dissolves into the aqueous fluid, leading to the increase of porosity, permeability, and the decrease of strength. The experimental results showed that the uniaxial compression strength of calcareous cemented arkosic sandstones drops by 60% after 20 days treatment with acid solution (Ning et al., 2003). Therefore, it is crucial to consider dissolution influence in the coupled THMC framework.

Although dissolution has been explored extensively for a long time, limited research has been done for dissolution in the THMC framework. Most existing THMC frameworks, when referring to 'reactive', only considered the influence of dissolution on the chemical transport or porosity/permeability alternation, but failed to consider the more important Mechanical-Chemical coupling process (Guimaraes et al., 2006; Zheng et al., 2010; Yin et al., 2011; Xiong et al., 2013; Nasir et al., 2014; Bea et al., 2016). The strong influence of chemical dissolution on stress-strain response has been observed by laboratory experiments (Amanullah et al., 1994; Qi et al., 2009; Ciantia et al., 2015; Momeni et al., 2017; Chen et al., 2020; Lin et al., 2020), the strength and mechanical properties of dissolved rock samples in unconfined compression test were much lower compared to the those of intact samples.

The mathematical modelling toward the Mechanical-Chemical coupling has been explored widely by the mechanics approach. Some research tried to reduce the mechanical properties, e.g. bulk modulus and shear modulus, to represent the chemical dissolution influence (Zhang et al., 2016), yet how the mechanical properties reduce was not discussed. Based on the principle of damage mechanics, Sun et al. (2020) and Fan et al. (2019) introduced the damage variable to reduce the mechanical properties. Similar research adopting damage mechanics also can be found in Gerard et al. (1998); Chen et al. (2007); Lyu et al. (2018). Unlike the above research, based on experimental results, Hu et al. (2012) and Jia et al. (2017) not only set the mechanical properties as functions of the introduced 'chemical damage variable', but also

embedded this variable into the stress-strain relationship. Tao et al. (2019) introduced a strain caused by the dissolution/precipitation from the solid matrix and defined the strain as the percentage of dissolved mineral volume against the total mineral volume. This method is more friendly and applicable in THMC research as the dissolved mineral volume can be estimated through geochemical kinetic modelling. However, he failed to explore deeper on this strain as it was only presented in the porosity change model.

An alternative way to study the reactive dissolution in the THMC framework is the thermodynamics approach and non-equilibrium thermodynamics approach, mainly by the mixture theory and its branches. For example, Kuhl et al. (2004) introduced a chemical internal variable to relate chemical reaction and mechanical damage Gawin et al. (2003); Gawin et al. (2008) developed a coupled HMC model to model the calcium leaching in cementitious material, in which the strength properties of chemically degraded material during the reactive transport process was proposed. Some researchers combined the mixture theory with non-equilibrium thermodynamics, and adopted the Clausius-Duhem Inequality (CDI) to explore the processes that contribute to the creation of entropy in a porous media through the balance law of mass, momentum, energy and entropy (Coussy, 1995; Coussy, 2004; Haxaire and Djeran-Maigre, 2009; Karrech, 2013; Zhang and Zhong, 2017b; Zhang and Zhong, 2018). Following the non-equilibrium thermodynamics concept, a thermodynamics variable, reaction extent, was introduced into the stress-strain relationship to describe the strain resulting from chemical reaction. The variable, reaction extent, is an important concept in geochemistry and can be estimated easily through geochemical kinetic modelling, making it a good choice for the chemical-mechanical modelling.

Although the CDI provides a powerful way to study the THMC coupling of a reactive mixture, the reaction type that the CDI deals with would be unclear. When modelling a reactive dissolution process, the CDI would only show the free energy change caused by the fluid but miss the free energy change by solid dissolving (discussed in section 3.2.1). This will hide the dissolution mechanism and make the reaction type unclear. Moreover, when using CDI, the derived stress-strain relation will always include a reaction extent term to represent the stress/strain induced by the reaction, no matter what kind of reaction it is. This is imprecise because when the reaction only takes place within the aqueous (or fluid phase such as gas) without changing the solid (for example, $CO_2 + H_2O \rightarrow H_2CO_3$), there could not be a

stress/strain produced directly on the solid matrix. Therefore, the constitutive relations would be imprecise if using CDI to deal with a reaction that occurs within the fluid without changing the solid.

In this paper, the non-equilibrium thermodynamics approach is adopted to develop the governing equations of coupled THMC process with reactive dissolution considered. Unlike most existing thermodynamics approaches exploring the dispassion energy through the Clausius-Duhem inequality, this paper focuses on Helmholtz free energy change of a dissolution system by quantifying the entropy production with the knowledge from non-equilibrium thermodynamics. Specifically, a new concept, solid affinity, is defined to describe the free energy change due to reactive mineral dissolution. The proposed approach overcomes the challenges in CDI.

The paper is arranged as: section 2 gives the basic mass and Helmholtz free energy balance equations; section 3 gives the CDI of a reacting system and illustrates the challenges of the CDI; section 4 quantifies the entropy production of a reactive dissolution system and takes the Helmholtz free energy as the research object, specifically, the concept 'solid affinity' is introduced to describe the free energy change of the solid due to dissolution; section 5 forms the constitutive relations of stress-strain and porosity under coupled reactive dissolution-THMC conduction; section 6 gives the hydraulic, chemical and thermal transport equations; section 7 uses numerical simulation to illustrate the role of dissolution in the coupled THMC framework by considering quartz dissolution.

2 Balance equation

2.1 Reaction extent and chemical affinity

For reactive dissolution, a general chemical reaction is considered as

$$\nu_x X_{(s)} + \nu_y Y_{(aq)} + \cdots \rightarrow \nu_z Z_{(aq)} + \cdots \tag{1}$$

in which ν_x, ν_y, ν_z are the stoichiometric coefficients for reactant X, Y and product Z.

Equation (1) describes a reactive dissolution that involves the dissolution of the solid mineral X, consumption of the aqueous component Y, generation of the aqueous component Z. It is easy to include more reactants and products in the reaction, but only limited items are listed in the reaction (1) for clarity and simplicity.

Let ξ be the extent of reaction, for any reactant or product i, the change in the number of moles per unit porous media volume is written as

$$\frac{dn_i}{V} = \chi v_i d\xi \tag{2}$$

where dn_i is the change in the number of moles, V is the volume of porous media; the symbol $\chi = -1$ for the reactant, $\chi = 1$ for the product, $\chi = 0$ if i does not join the reaction.

The affinity A, which is the driving force of the reaction, is defined as (Kondepudi and Prigogine, 2014)

$$A = -\sum \chi v_i M^i \mu^i = v_x M^X \mu^X + v_y M^Y \mu^Y - v_z M^Z \mu^Z \tag{3}$$

where M^i, μ^i are the molar mass and chemical potential of reactant or product i, respectively.

2.2 Mass balance equations

Let α represents any constituent (solid, water, or aqueous chemicals) in the mixture. The general mass balance equation for α can be written as

$$\frac{D}{Dt}\left(\int_V \rho^\alpha dV\right) = -\int_S \mathbf{I}^\alpha \cdot \mathbf{n} dS + \int_V \chi v_\alpha M^\alpha \dot{\xi} dV \tag{4}$$

in which ρ^α, $\mathbf{I}^\alpha$ and M^α are the density, flux, and molar mass of constituent α. $\mathbf{n}$ is the outward unit normal vector; $\chi = -1$ for reactant, $\chi = 1$ for product, $\chi = 0$ if α does not join the reaction. If α does not flow out through the boundary S, for example, the solid mineral, then $\mathbf{I}^\alpha = 0$.

The material time derivative following the motion of the solid is $\frac{d(\cdot)}{dt} = \frac{\partial(\cdot)}{\partial t} + \mathbf{v}^s \cdot \nabla(\cdot)$, then, equation (4) can be written as

$$\dot{\rho}^\alpha + \rho^\alpha \nabla \cdot \mathbf{v}^s + \nabla \cdot \mathbf{I}^\alpha = \chi v_\alpha M^\alpha \dot{\xi} \tag{5}$$

in which $\mathbf{v}^s$ is the velocity of the solid.

2.3 Helmholtz free energy balance equation

Helmholtz free energy measures the useful work, and is defined as the difference between internal energy and entropy (Hasse.R, 1969). Hence, the balance equation for Helmholtz free energy can be derived through the balance equation of internal energy and balance equation of

entropy. This section takes the free energy balance derivation from Ma et al. (2022)

2.3.1 Internal energy balance

The internal energy change considered is only the mechanical work and heat exchange. Neglecting the heat change by chemical reaction or any other point source, the internal energy balance equation is

$$\frac{D}{Dt}\int_V \varepsilon dV = \int_S (\boldsymbol{\sigma}\mathbf{v}^s \cdot \mathbf{I}'_q)\cdot \mathbf{n} dS - \int_S \sum h^\alpha \mathbf{I}^\alpha \cdot \mathbf{n} dS \tag{6}$$

Its local form is

$$\dot{\varepsilon} + \varepsilon \nabla \cdot \mathbf{v}^s - \nabla \cdot (\boldsymbol{\sigma}\mathbf{v}^s) + \nabla \cdot \mathbf{I}'_q + \nabla \cdot \sum h^\alpha \mathbf{I}^\alpha = 0 \tag{7}$$

where ε is the internal energy density, $\boldsymbol{\sigma}$ is the Cauchy stress tensor, h^α is the enthalpy of mass α, $\mathbf{I}'_q = \mathbf{q} - \sum h^\alpha \mathbf{I}^\alpha$ is the reduced heat flow, which is the difference between the total heat flow $\mathbf{q}$ and the heat flow carried by mass flow $\sum h^\alpha \mathbf{I}^\alpha$.

2.3.2 entropy balance

The entropy change includes the entropy exchange with the surroundings $\mathbf{I}_\eta$ and the entropy generated inside the porous media γ, and the balance equation for entropy is

$$\frac{D}{Dt}\int_V \eta^{mix} dV = -\int_S \mathbf{I}_\eta \cdot \mathbf{n} dS + \int_V \gamma dV$$

The local form is

$$\dot{\eta}^{mix} + \eta^{mix}\nabla \cdot \mathbf{v}^s + \nabla \cdot \mathbf{I}_\eta - \gamma = 0 \tag{8}$$

in which η^{mix} is the entropy density of the mixture system, which includes the entropy of all the constituents in the mixture; γ is the entropy produced per unit volume. $\mathbf{I}_\eta$ is the entropy exchange with the surroundings, which can be written as (Katchalsky and Curran, 1965)

$$\mathbf{I}_\eta = \frac{\mathbf{q} - \sum \mu^\alpha \mathbf{I}^\alpha}{T} = \frac{\mathbf{I}'_q}{T} + \sum \eta^\alpha \mathbf{I}^\alpha \tag{9}$$

In equation (9), T is the temperature and the relationship $\mu^\alpha = h^\alpha - T\eta^\alpha$ is used.

2.3.3 Helmholtz free energy balance equation

From the definition of Helmholtz free energy density $\psi = \varepsilon - T\eta^{mix}$, using material time derivative leads to the Helmholtz free energy density relationship in local form as

$$\dot{\psi} + \psi \nabla \cdot \mathbf{v}^s = \dot{\varepsilon} + \varepsilon \nabla \cdot \mathbf{v}^s - \left(\dot{T} + T\nabla \cdot \mathbf{v}^s\right)\eta^{mix} - T\left(\dot{\eta}^{mix} + \eta^{mix}\nabla \cdot \mathbf{v}^s\right) \tag{10}$$

Then, from the internal energy equation (7) and the entropy equation (8), the balance equation for Helmholtz free energy density is

$$\dot{\psi}+\psi\nabla\cdot\mathbf{v}^s-\nabla\cdot(\boldsymbol{\sigma}\mathbf{v}^s)+\nabla\cdot\mathbf{I}'_q+\nabla\cdot\sum h^\alpha\mathbf{I}^\alpha+\left(\dot{T}+T\nabla\cdot\mathbf{v}^s\right)\eta^{mix}-T\nabla\cdot\mathbf{I}_\eta=-T\gamma\le 0 \quad (11)$$

3 Challenge in Clausius-Duhem inequality

3.1 Clausius-Duhem inequality

The right hand of equation (11), $\Phi=T\gamma$, is the overall dispassion energy caused by the irreversible heat and mass transport, as well as chemical reaction. Invoking the entropy flux equation (9) into equation (11), the general CDI can be obtained as

$$\Phi=T\gamma$$

$$=\underbrace{\nabla\cdot(\boldsymbol{\sigma}\mathbf{v}^s)-\left(\dot{\psi}+\psi\nabla\cdot\mathbf{v}^s\right)-\eta^{mix}\left(\dot{T}+T\nabla\cdot\mathbf{v}^s\right)-\sum\mu^\alpha\nabla\cdot\mathbf{I}^\alpha}_{\Phi_1}\underbrace{-\frac{\mathbf{q}}{T}\cdot\nabla T}_{\Phi_2}\underbrace{-T\sum\mathbf{I}^\alpha\cdot\nabla\frac{\mu^\alpha}{T}}_{\Phi_3}\ge 0 \quad (12)$$

Equation (12) is the general form of the CDI, which is the same as the one given in section 3.2.3 in Coussy (2004) if considering the flux of solid to be zero. Φ_1 is the skeleton dispassion, which accounts for the dispassion related to the sole skeleton; Φ_2 is the thermal dispassion; $\Phi_3=T\sum\mathbf{I}^\alpha\cdot\nabla\frac{\mu^\alpha}{T}=T\sum_{\alpha\in f}\mathbf{I}^\alpha\cdot\nabla\frac{\mu^\alpha}{T}$ is the fluid dispassion, where $\alpha\in f$ denotes the pore fluid constituents.

Let us focus attention on Φ_1, which is used to develop the mechanical constitutive relationship. The term $-\mu^\alpha\nabla\cdot\mathbf{I}^\alpha$ represents the energy dispassion by mass change. From the mass balance equation (5), there must be $-\mu^\alpha\nabla\cdot\mathbf{I}^\alpha=\mu^\alpha\left(\dot{\rho}^\alpha+\rho^\alpha\nabla\cdot\mathbf{v}^s\right)-\mu^\alpha\chi v_\alpha M^\alpha\dot{\xi}$, then Φ_1 becomes

$$\Phi_1=\nabla\cdot(\boldsymbol{\sigma}\mathbf{v}^s)-\left(\dot{\psi}+\psi\nabla\cdot\mathbf{v}^s\right)-\eta^{mix}\left(\dot{T}+T\nabla\cdot\mathbf{v}^s\right)+\sum u^\alpha\left(\dot{\rho}^\alpha+\rho^\alpha\nabla\cdot\mathbf{v}^s\right)+A\dot{\xi} \quad (13)$$

where $A=-\sum\chi v_\alpha M^\alpha\mu^\alpha$ is the affinity of the reaction.

The CDI (13) is widely adopted to explore a reacting system as the term $A\dot{\xi}$ represents reaction (Coussy, 1995; Coussy, 2004; Haxaire and Djeran-Maigre, 2009; Karrech, 2013; Zhang and Zhong, 2017b; Zhang and Zhong, 2017a; Zhang and Zhong, 2018). However, the above research does not give a detailed reaction formula or specify a reaction type, as a result, they

failed to explore the mechanism. The next section will show when considering a reactive dissolution, the CDI will encounter some challenges.

3.2 Challenges in Clausius-Duhem Inequality

3.2.1 Unclear reaction type and hidden mechanism

When CDI (13) is used to deal with a dissolution process, for example, reactive dissolution (1), it becomes

$$\begin{aligned}\Phi_1 = {} & \nabla\cdot(\boldsymbol{\sigma}\mathbf{v}^s) - \left(\dot{\psi} + \psi\nabla\cdot\mathbf{v}^s\right) - \eta^{mix}\left(\dot{T} + T\nabla\cdot\mathbf{v}^s\right) \\ & + \mu^X\left(\dot{\rho}^X + \rho^X\nabla\cdot\mathbf{v}^s\right) + \sum_{\alpha\in f} u^\alpha\left(\dot{\rho}^\alpha + \rho^\alpha\nabla\cdot\mathbf{v}^s\right) + \left(v_x M^X\mu^X + v_y M^Y\mu^Y - v_z M^Z\mu^Z\right)\dot{\xi}\end{aligned} \tag{14}$$

Since there is normally no solid mass flux across the boundary, therefore $\mathbf{I}^X = 0$. From the mass balance (5), there must be $\mu^X\left(\dot{\rho}^X + \rho^X\nabla\cdot\mathbf{v}^s\right) + v_x M^X\mu^X\dot{\xi} = 0$, then equation (14) becomes

$$\begin{aligned}\Phi_1 = {} & \nabla\cdot(\boldsymbol{\sigma}\mathbf{v}^s) - \left(\dot{\psi} + \psi\nabla\cdot\mathbf{v}^s\right) - \eta^{mix}\left(\dot{T} + T\nabla\cdot\mathbf{v}^s\right) \\ & + \sum_{\alpha\in f} u^\alpha\left(\dot{\rho}^\alpha + \rho^\alpha\nabla\cdot\mathbf{v}^s\right) + \left(v_y M^Y\mu^Y - v_z M^Z\mu^Z\right)\dot{\xi}\end{aligned} \tag{15}$$

where $v_y M^Y\mu^Y - v_z M^Z\mu^Z$ is the contribution of the fluid parts to the chemical affinity (3).

Although equation (15) represents the reactive dissolution (1), it only shows the energy dispassion caused by the change of aqueous constituents, including the reactant Y and product Z, but it misses the energy dispassion by solid mineral X dissolving. The key feature of dissolution is the solid mass change and corresponding free energy change, which is not represented in CDI (15). Therefore, CDI (15) hides the dissolution mechanics. It can be estimated that, for any reaction interacting with the solid, like precipitation and sorption, the mechanism would be hidden.

Meanwhile, if just looking at equation (15) without going through the derivation steps, the readers would be confused about what type of reaction it is dealing with. Since the dissolution mechanism is hidden, the reaction type in equation (15) would be unclear, as it can be regarded as either a dissolution reaction or a reaction just between aqueous constituents Y and Z only.

Although equation (14) has the terms indicating the solid energy change by dissolution, e.g. $\mu^X\left(\dot{\rho}^X+\rho^X\nabla\cdot\mathbf{v}^s\right)+\left(v_x M^X\mu^X\right)\dot{\xi}$, it is not used for the final derivation. This is because, if using equation (14), due to the presence of $\mu^X\left(\dot{\rho}^X+\rho^X\nabla\cdot\mathbf{v}^s\right)$, the final constitute equation must contains u^X, ρ^X as state variables. The chemical potential u^X and its relationship with other state variables are difficult to determine, which would restrict the application of the derived equations (see Zhang and Zhong (2017b); Zhang and Zhong (2017a); Zhang and Zhong (2018)). If using equation (15), the term $u^\alpha\left(\dot{\rho}^\alpha+\rho^\alpha\nabla\cdot\mathbf{v}^s\right)$ could be converted into $p\dot{\phi}$ to switch the state variables u^α and ρ^α into pressure p and porosity ϕ (see Coussy (2004); Haxaire and Djeran-Maigre (2009); Karrech (2013)).

3.2.2 Imprecise constitutive result

If the reaction takes place within the fluid only without changing the solid, for example $CO_2+H_2O\rightarrow H_2CO_3$, then, CDI (13) becomes:

$$\Phi_1=\nabla\cdot(\boldsymbol{\sigma}\mathbf{v}^s)-\left(\dot{\psi}+\psi\nabla\cdot\mathbf{v}^s\right)-\eta^{mix}\left(\dot{T}+T\nabla\cdot\mathbf{v}^s\right)+\sum_{\alpha\in f}u^\alpha\left(\dot{\rho}^\alpha+\rho^\alpha\nabla\cdot\mathbf{v}^s\right)+A\dot{\xi} \quad (16)$$

where the term $A\dot{\xi}$ represents the energy dispassion caused by the reaction occurs within the fluid.

Since there is a variable $\dot{\xi}$ in CDI (16), a new term, like $-H_{ij}\dot{\xi}$ in equation (36), must be introduced into the stress-strain relationship. This term is explained as 'as the chemical extent increases by quantity $\dot{\xi}$, the chemical reaction produces the strain $-H_{ij}\dot{\xi}$' (Coussy, 2004). However, if the reaction does not change the solid, it could not generate a stress/strain directly on the solid matrix, and there should not be a $-H_{ij}\dot{\xi}$ term in the developed stress-strain constitutive relationship. Therefore, if the reaction occurs within the fluid only, the use of CDI would generate imprecise constitutive equations.

Consider a reaction occurring within the fluid only: $\nu_y Y_{(aq)}+\cdots\rightarrow\nu_z Z_{(aq)}+\cdots$, of which the affinity is $A=\left(v_y M^Y\mu^Y-v_z M^Z\mu^Z\right)\dot{\xi}$. For such a reaction, the CDI (16) will become the same as CDI (15). This further strengthens the unclear reaction type and hidden mechanism

challenge described in section 3.1 as totally different reaction types hole the same CDI descriptions.

4 Helmholtz free energy change in a dissolution process

4.1 Entropy production

In this section, the Helmholtz free energy change in a dissolution process is taken as the research object. The starting point is the Helmholtz free energy balance equation (11). It is noticed that the entropy production $T\gamma$ can be quantified with the knowledge from non-equilibrium thermodynamics as (Katchalsky and Curran, 1965),

$$0 \le T\gamma = -\mathbf{I}_\eta \cdot \nabla T - \sum \mathbf{I}^\alpha \cdot \nabla \mu^\alpha + A\dot{\xi} \tag{17}$$

In equation (17), the terms on the right hand of the equality are: 1. $-\mathbf{I}_\eta \cdot \nabla T = -\left(\frac{\mathbf{q} - \sum \mu^\alpha \mathbf{I}^\alpha}{T} \right) \cdot \nabla T = -\left(\frac{\mathbf{I}'_q}{T} + \sum \eta^\alpha \mathbf{I}^\alpha \right) \cdot \nabla T$, the entropy production caused by heat exchange, including heat convection and heat advection; 2. $-\sum \mathbf{I}^\alpha \cdot \nabla \mu^\alpha$, the entropy production caused by mass flow; 3. $A\dot{\xi}$, the entropy production caused by chemical reaction.

4.2 Helmholtz free energy change

Combine equations (17) and (11), the Helmholtz free energy change can be rewritten as

$$\dot{\psi} + \psi \nabla \cdot \mathbf{v}^s = \left(\boldsymbol{\sigma} : \nabla \mathbf{v}^s \right) - \left(\dot{T} + T \nabla \cdot \mathbf{v}^s \right) \eta^{mix} - \sum u^\alpha \nabla \cdot \mathbf{I}^\alpha - A\dot{\xi} \tag{18}$$

Using mass balance equation (5), equation (18) can be converted into:

$$\dot{\psi} + \psi \nabla \cdot \mathbf{v}^s = \left(\boldsymbol{\sigma} : \nabla \mathbf{v}^s \right) - \left(\dot{T} + T \nabla \cdot \mathbf{v}^s \right) \eta^{mix} + \sum \left(\mu^\alpha \dot{\rho}^\alpha + \mu^\alpha \rho^\alpha \nabla \cdot \mathbf{v}^s - \mu^\alpha \chi v_\alpha M^\alpha \dot{\xi} \right) - A\dot{\xi} \tag{19}$$

For the reactive dissolution (1), from the expression of affinity (3), and considering the density of unreacted solid does not change, equation (19) could be reduced to

$$\dot{\psi} + \psi \nabla \cdot \mathbf{v}^s = \left(\boldsymbol{\sigma} : \nabla \mathbf{v}^s \right) - \left(\dot{T} + T \nabla \cdot \mathbf{v}^s \right) \eta^{mix} + \sum_{\alpha \in f} \left(\mu^\alpha \dot{\rho}^\alpha + \mu^\alpha \rho^\alpha \nabla \cdot \mathbf{v}^s \right) - v_x M^X \mu^X \dot{\xi} \tag{20}$$

It can be found that $v_a M^A \mu^A$ is the contribution of the solid part in the affinity equation (3). To better describe the free energy change by dissolution, a new concept, solid affinity, is defined as

$$A_s = v_x M^X \mu^X \tag{21}$$

Equation (20) becomes

$$\dot{\psi}+\psi\nabla\cdot\mathbf{v}^s=\left(\boldsymbol{\sigma}:\nabla\mathbf{v}^s\right)-\left(\dot{T}+T\nabla\cdot\mathbf{v}^s\right)\eta^{mix}+\sum_{\alpha\in f}\left(\mu^\alpha\dot{\rho}^\alpha+\mu^\alpha\rho^\alpha\nabla\cdot\mathbf{v}^s\right)-A_s\dot{\xi} \quad (22)$$

The term $-A_s\dot{\xi}$ represents the Helmholtz free energy change of the solid due to reactive dissolution. If the reaction is a precipitation or sorption process, it can be estimated that a similar term will be added into equation (22); if the reaction takes place within the fluid/gas phase without changing the solid, then A_s vanishes. Therefore, using equation (22) to derive the constitutive equations, the reaction type can be specified through $A_s\dot{\xi}$, the dissolution mechanism can be presented by $A_s\dot{\xi}$ and the constitutive relationship can be precise if $A_s\dot{\xi}$ vanishes.

Remark: when converting equation (19) into (20), an alternative form of equation (20) can be obtained as

$$\dot{\psi}+\psi\nabla\cdot\mathbf{v}^s=\left(\boldsymbol{\sigma}:\nabla\mathbf{v}^s\right)-\left(\dot{T}+T\nabla\cdot\mathbf{v}^s\right)\eta^{mix}+\sum_{\alpha\in f}\left(\mu^\alpha\dot{\rho}^\alpha+\mu^\alpha\rho^\alpha\nabla\cdot\mathbf{v}^s\right)+\left(\mu^X\dot{\rho}^X+\mu^X\rho^X\nabla\cdot\mathbf{v}^s\right) \quad (23)$$

This form can also be obtained from (22) by using the mass balance equation. Equation (23) indicating that the change of Helmholtz free energy can be described by the change of all mass. If using equation (23) for the final derivation, the variable adopted will be density, instead of reaction extent. One can also adopt porosity as a variable for later derivation as the porosity change can be directly linked to the density change or reaction extent.

5 Constitutive relations

5.1 Helmholtz free energy in the reference configuration

Some basic concept from continuum mechanics are adopted (Wriggers, 2008):

$$\mathbf{F}=\frac{\partial\mathbf{x}^s}{\partial\mathbf{X}^s}(\mathbf{X}^s,t),\ \mathbf{E}=\frac{1}{2}(\mathbf{F}^{\mathrm{T}}\mathbf{F}-1),\ \mathbf{T}=J\mathbf{F}^{-1}\boldsymbol{\sigma}\mathbf{F}^{-T},\ J=\frac{dV}{dV_0},\ \dot{J}=J\nabla\cdot\mathbf{v}^s \quad (24)$$

where $\mathbf{F}$, $\mathbf{E}$, $\mathbf{T}$ are the solid deformation, the Green strain and the second Piola-Kirchhoff stress, respectively; J is the determinant of $\mathbf{F}$, which determines the volume change of the volume defined by the solid boundary, dV is the volume in the current configuration, and dV_0 is the volume of the reference configuration.

Using the in continuum mechanics, the Helmholtz free energy equation (22) can be converted

to the reference configuration as

$$\dot{\Psi} = tr(\mathbf{T}\dot{\mathbf{E}}) - \mathrm{H}^{mix}\dot{T} + \sum_{\alpha \in f} \mu^{\alpha} \dot{m}^{\alpha} - A_s \dot{\xi} \tag{25}$$

in which

$$\Psi = J\psi \ , \ m^{\alpha} = J\rho^{\alpha} \ , \ \mathrm{H}^{mix} = J\eta^{mix} \ , \ \xi = J\xi \tag{26}$$

Ψ is the free energy in the reference configuration and m^{α} is the mass density of the pore fluid component α in the reference configuration, H^{mix} is the entropy density of the mixture in the reference configuration, ξ is the reaction extent in the reference configuration (the kinetic energy of ξ is not considered).

5.2 Helmholtz free energy density of pore space

The free energy density of the pore space ψ_{pore} can be obtained from classical thermodynamics

$$\psi_{pore} = -p^{f} + \eta_f^f T + \sum_{\alpha \in f} \rho_f^{\alpha} u^{\alpha} \tag{27}$$

where p^f is the pore fluid pressure, η_f^f is the pore fluid entropy per unit volume fluid, ρ_f^{α} is the mass density of fluid component α, relative to the volume pore fluid.

According to the Gibbs-Duhem equation, for the pore fluid, there is

$$\dot{p}^{f} = \eta_f^f \dot{T} + \sum_{\alpha \in f} \rho_f^{\alpha} \dot{u}^{\alpha} \tag{28}$$

Invoking (28) into the time derivation of equation (27), it leads to

$$\dot{\psi}_{pore} = T\dot{\eta}_f^f + \sum_{\alpha \in f} \dot{\rho}_f^{\alpha} u^{\alpha} \tag{29}$$

5.3 Helmholtz free energy of the solid

The free energy of the solid matrix is the difference between total free energy and free energy in the pore space. By subtracting the contribution of $\phi\psi_{pore}$ due to the pore fluid from the free energy Ψ, the free energy of the solid matrix Ψ_s is

$$\Psi_s = \Psi - J\phi\psi_{pore} \tag{30}$$

where $\upsilon = J\phi$ is denoted as pore volume per unit referential volume.

From equation (25), (29) and (27), the change of Ψ_s can be written as a function of $\mathbf{E}, \upsilon, \xi, T$:

$$\dot{\Psi}_s\left(\mathbf{E},\upsilon,\xi,T\right)=tr\left(\mathbf{T}\dot{\mathbf{E}}\right)+p^f\dot{\upsilon}-A_s\dot{\xi}-\mathrm{H}^s\dot{T} \tag{31}$$

where $\mathrm{H}^s=\mathrm{H}^{mix}-\upsilon\eta_f^f$ is the entropy density of the solid.

5.4 Incremental law

Equation (31) takes $\mathbf{E}$, υ, ξ, T as the state variable. Define W as:

$$W=\Psi_s-p^f\upsilon \tag{32}$$

Adopting Legendre transforms, there is

$$\dot{W}\left(\mathbf{E},p^f,\xi,T\right)=tr\left(\mathbf{T}\dot{\mathbf{E}}\right)-\upsilon\dot{p}^f-A_s\dot{\xi}-\mathrm{H}^s\dot{T} \tag{33}$$

Equation (33) takes $\mathbf{E}$, p^f, ξ, T as the state variables and links to their conjugate thermodynamics state variable $\mathbf{T}$, υ, A_s, H^s

Equation (33) must have:

$$T_{ij}=\left(\frac{\partial W}{\partial E_{ij}}\right)_{p^f,\xi,T},\ \upsilon=-\left(\frac{\partial W}{\partial p^f}\right)_{E_{ij},\xi,T},\ A_s=-\left(\frac{\partial W}{\partial \xi}\right)_{E_{ij},p^f,T},\ \eta^s=-\left(\frac{\partial W}{\partial T}\right)_{E_{ij},p^f,\xi} \tag{34}$$

So that:

$$\dot{W}(\mathbf{E},p^f,\xi,T)=\left(\frac{\partial W}{\partial E_{ij}}\right)_{p^f,\xi,T}\dot{E}_{ij}+\left(\frac{\partial W}{\partial p^f}\right)_{E_{ij},\xi,T}p^f+\left(\frac{\partial W}{\partial A_s}\right)_{E_{ij},p^f,T}\dot{\xi}+\left(\frac{\partial W}{\partial T}\right)_{E_{ij},p^f,\xi}\dot{T} \tag{35}$$

Differentiated equation (34), the fundamental incremental constitutive equations for the stress, pore volume fraction, solid affinity and entropy density of the solid can be obtained as

$$dT_{ij}=L_{ijkl}dE_{kl}-M_{ij}dp^f-H_{ij}d\xi-F_{ij}dT \tag{36}$$

$$d\upsilon=M_{ij}dE_{ij}+Qdp^f+Dd\xi+NdT \tag{37}$$

$$dA_s=H_{ij}dE_{ij}+Ddp^f+Yd\xi+UdT \tag{38}$$

$$d\mathrm{H}^s=F_{ij}dE_{ij}+Ndp^f+Ud\xi+VdT \tag{39}$$

where $L_{ijkl}, M_{ij}, S_{ij}, H_{ij}, F_{ij}, Q, B^\beta, D, N, Z^\beta, X^\beta, R^\beta, Y, U, V$ are coefficients

As the paper introduces the solid affinity A_s to describes the Helmholtz free energy change, the cross coupling group equations (36)-(39) are different from other research in that equation (38) presents the solid affinity change instead of the overall affinity change.

5.5 Linear isotropic response of stress and porosity

The equations (36)-(39) represent the evolution of the Piola-Kirchhoff stress T_{ij}, porosity υ, solid affinity A_s and solid entropy H^s with Green Strain tensor E_{ij}, pore fluid pressure p^f, reaction extent ξ and temperature T. These equations are rather general because the stress T_{ij} applies to all kinds of situations, including large strain, anisotropy, etc. To obtain the governing equations, the mechanical behaviour is restrained to be in small strain and isotropic condition, so that the Green Strain tensor E_{ij} and the Piola-Kirchhoff stress T_{ij} can be substituted by strain tensor ε_{ij} and Cauchy stress σ_{ij}; and further assume the material to be symmetric and isotropic, so that so that the tensor M_{ij}, H_{ij} and F_{ij} can be replaced by a scalar coefficient with Kronecker delta δ_{ij}:

$$T_{ij} = \sigma_{ij},\ E_{ij} = \varepsilon_{ij},\ M_{ij} = \zeta\delta_{ij},\ H_{ij} = \omega_r\delta_{ij},\ F_{ij} = \omega_T\delta_{ij} \tag{40}$$

For elastic deformation of soil/rock, then, the stiffness L_{ijkl} can be written in a form of a fourth-order isotropic tensor

$$L_{ijkl} = G(\delta_{ik}\delta_{jl} + \delta_{il}\delta_{jk}) + (K - \frac{2G}{3})\delta_{ij}\delta_{kl} \tag{41}$$

where G, K are the shear modulus and bulk modulus.

5.5.1 Stress response

Based on the assumption and relationships in equation (40) and equation (41), and further assume $J = 1$, the stress evolution equation (36) becomes

$$d\sigma_{ij} = (K - \frac{2G}{3})d\varepsilon_{kk}\delta_{ij} + 2Gd\varepsilon_{ij} - \zeta dp^f\delta_{ij} - \omega_R d\xi\delta_{ij} - \omega_T dT\delta_{ij} \tag{42}$$

where $\zeta = 1-(K/K_s)$ is the Biot coefficient, K and K_s are the bulk modulus of the porous media and the solid grain; $\omega_T = K\alpha_s$ with α_s being the thermal expansion coefficient of the solid;

In equation (42), the term $-\omega_R\dot{\xi}\delta_{ij}$ represents the stress change by reactive dissolution, like the thermal term, it can be written as $-K\omega_r\dot{\xi}\delta_{ij}$, in which $-\omega_r\dot{\xi}\delta_{ij}$ representing the strain induced

by dissolution. According to Tao et al. (2019), the volumetric strain caused by chemical dissolution is

$$d\left(\varepsilon_d\right)=\frac{V_s^{rem}}{V_s^{ini}}-1=-\frac{M_X}{\rho_t^X}\frac{d\left(n_X\right)}{V_s}=-V_{m,X}\frac{1}{1-\phi}d\xi \tag{43}$$

where V_s is the volume of the solid part, $V_{m,X}=\frac{M_X}{\rho_t^X}$ is the molar volume of mineral X. The stress equation (42) can then be written as

$$d\sigma_{ij}=(K-\frac{2G}{3})d\varepsilon_{kk}\delta_{ij}+2Gd\varepsilon_{ij}-\zeta dp^f\delta_{ij}-K\frac{V_{m,X}}{1-\phi}d\xi\delta_{ij}-K\alpha_s dT\delta_{ij} \tag{44}$$

Or converted into a strain form as

$$d\varepsilon_{ij}=\frac{1}{2G}d\sigma_{ij}-\frac{1}{2G}\frac{\theta}{1+\theta}d\sigma_{kk}\delta_{ij}+\frac{\zeta}{K}dp^f\delta_{ij}+\frac{V_{m,X}}{1-\phi}d\xi\delta_{ij}+\alpha_s dT\delta_{ij} \tag{45}$$

5.5.2 Porosity

Taking the assumption made before, the porosity evolution can be reduced from equation (37) as

$$d\upsilon=\zeta d\varepsilon_{ii}+Qdp^f+Dd\xi+NdT \tag{46}$$

where the coefficients are $Q=(1/K_s)(\zeta-\phi)$ and $N=\left(\phi-\zeta\right)\alpha_s$.

Since ξ denotes the change in number of moles per unit mixture volume, the pore volume change by dissolution can be obtained as

$$D=M_X/\rho_t^X \tag{47}$$

Then, the porosity evolution equation can be rewritten as

$$d\upsilon=\zeta d\varepsilon_{ii}+\frac{\zeta-\phi}{K_s}dp^f+V_{m,X}d\xi+\left(\phi-\zeta\right)\alpha_s dT \tag{48}$$

6 Transport equation

6.1 Hydraulic transport

The balance equation for the pore fluid as a whole is

$$\frac{D}{Dt}\left(\int_V\rho^f dV\right)=-\sum_{\beta\in f}\int_S\mathbf{I}^f\cdot\mathbf{n}dS+\sum_{\beta\in f}\int_V\chi v_\alpha M^\alpha\dot{\xi}dV \tag{49}$$

From the mass balance equation (5), the balance equation for the pore fluid as a whole is

$$\dot{\rho}^f + \rho^f \nabla \cdot \mathbf{v}^s + \nabla \cdot \mathbf{I}^f = \sum_{\beta \in f} \chi v_\alpha M^\alpha \dot{\xi} \tag{50}$$

where ρ^f is the density of the pore fluid, which is defined as the mass of fluid over the volume of the porous media; $\mathbf{I}^f = \rho^f (\mathbf{v}^f - \mathbf{v}^s)$ is the flux of pore fluid.

The density ρ^f can be linked to ρ_f^f, which is defined as the mass of fluid over the volume of the fluid, through

$$\rho^f = \phi \rho_f^f \tag{51}$$

Since the Darcy velocity is defined as

$$\mathbf{u} = \phi(\mathbf{v}^f - \mathbf{v}^s) \tag{52}$$

From equation (51), and the relationship of J in equation (24), the mass balance equation (50) can be rewritten as

$$\left(\upsilon \rho_f^f\right)^{\square} + J \nabla \cdot \left(\rho_f^f \mathbf{u}\right) = J \sum_{\beta \in f} \chi v_\alpha M^\alpha \dot{\xi} \tag{53}$$

The fluid density change under coupled THMC condition can be regarded as a function of pressure and temperature $\rho_f^f = \rho_f^f \left(p^f, T\right)$ (Hosking et al., 2020):

$$\dot{\rho}_f^f (T, p^f) = \rho_f^f \left(\frac{1}{K_f} \dot{p}^f - \alpha_f \dot{T} \right) \tag{54}$$

in which $K_f = \frac{1}{\rho_f^f} \left(\frac{\partial \rho_f^f}{\partial p^f} \right)_T$ is the bulk modulus of the fluid, $\alpha_f = -\frac{1}{\rho_f^f} \left(\frac{\partial \rho_f^f}{\partial T} \right)_{p^f}$ is the thermal expansion coefficient of the fluid.

Invoking the density function (54) and the porosity evolution equation (48) into equation (53), and assuming that $J = 1$, neglecting the space variation of fluid density, i.e. $\nabla \cdot \rho_f^f = 0$, the governing equation for fluid transport with consideration of the reactive dissolution (1) can be obtained as

$$\zeta \dot{\varepsilon}_{ii} + \nabla \cdot \mathbf{u} + \left(\frac{\phi}{K_f} + \frac{\zeta - \phi}{K_s} \right) \dot{p}^f + \left((\phi - \zeta) \alpha_s - \phi \alpha_f \right) \dot{T} + V_{m,X} \dot{\xi} = \frac{\left(-v_y M^Y + v_z M^Z \right) \dot{\xi}}{\rho_f^f} \tag{55}$$

6.2 Chemical transport

Any chemical k in the pore fluid obeys the similar relations with (51), i.e. $\rho^k = \phi\rho_f^k$, therefore, from mass balance equation (5), there is

$$\left(\upsilon\rho_f^k\right)^{\square} + J\nabla\cdot\mathbf{I}^k = J\chi v_k M^k\dot{\xi} \tag{56}$$

where ρ_f^k is the density of chemical k, which is defined against the volume of the pore fluid. The diffusion flux $\mathbf{J}^k = \rho^k(\mathbf{v}^k - \mathbf{v}^f)$ of the chemical k, which is relative to the barycentric motion, can be linked to Darcy flux through

$$\mathbf{J}^k = \mathbf{I}^k - \rho_f^k\mathbf{u} \tag{57}$$

Then, equation (56) can be rewritten as

$$\left(\phi\rho_f^k\right)^{\square} + J\nabla\cdot\mathbf{J}^k + J\nabla\cdot\left(\rho_f^k\mathbf{u}\right) = J\chi v_k M^k\dot{\xi} \tag{58}$$

In the transport research, the fluid could be assumed to be incompressible. If the mass fraction of chemical k is defined as $w^k = \rho_f^k/\rho_f^f$, then equation (58) can be written as

$$\left(\phi w^k\rho_f^f\right)^{\square} + J\nabla\cdot\mathbf{J}^k + J\nabla\cdot\left(w^k\rho_f^f\mathbf{u}\right) = J\chi v_k M^k\dot{\xi} \tag{59}$$

Summarising all chemicals, it can be found $\sum\mathbf{J}^k = 0$ and $\sum w^k = 1$, then, based on equation (59), summing over all fluid components leads to

$$\left(\phi\rho_f^f\right)^{\square} + J\nabla\cdot\left(\rho_f^f\mathbf{u}\right) = \sum_k J\chi v_k M^k\dot{\xi} \tag{60}$$

Invoking equation (60) into (59), and assuming $J = 1$, the chemical transport governing equation can be obtained

$$\phi\rho_f^f\dot{w}^k + \nabla\cdot\mathbf{J}^k + \rho_f^f\mathbf{u}\cdot\nabla w^k = \chi v_k M^k\dot{\xi} - w^k\sum_k\chi v_k M^k\dot{\xi} \tag{61}$$

6.3 Thermal transport

Take all the solid constituent as a whole and all pore fluid as a whole, the heat balance equation of the mixture can be written as

$$\frac{D}{Dt}\int_V\left(q^s + q^f\right)dV = -\int_S(\mathbf{I}_q' + h^f\mathbf{I}^f)\cdot\mathbf{n}dS + \dot{Q} \tag{62}$$

where $q^s = \rho^s C^s T$, $q^f = \rho^f C^f T$ are the heat densities of the solid and the pore fluid, C^s, C^f are the specific heat capacity; h^f and $\mathbf{I}^f$ are the enthalpy and flux of pore fluid, $\dot{Q}$ represents

any other point source or heat change by chemical reaction.

The material time derivative of equation (62) is

$$\left(\dot{q}^s + \dot{q}^f\right) + \left(q^s + q^f\right)\nabla\cdot\mathbf{v}^s + \nabla\cdot\mathbf{I}'_q + \nabla\cdot h^f\mathbf{I}^f = \dot{Q} \tag{63}$$

Similar to the mass density relationship (51), the heat density q^s, q^f (relative to the volume of the porous media) can be linked to heat density q_s^s, q_f^f (relative to the volume of the solid and the pore fluid) through

$$q^s = (1-\phi)q_s^s = \phi^s\rho_s^s C^s T,\ q^f = \phi q_f^f = \phi\rho_f^f C^f T \tag{64}$$

Then, equation (63) can be converted to

$$\left((J-\upsilon)\rho_s^s C^s T\right)^{\square} + \left(S^f\upsilon\rho_f^f C^f T\right)^{\square} + J\nabla\cdot\mathbf{I}'_q + J\nabla\cdot h^f\mathbf{I}^f = J\dot{Q} \tag{65}$$

Assuming $J=1$, and considering $\mathbf{I}'_q = -\lambda\nabla T$, $\mathbf{q}_f = h^f\mathbf{I}^f = \rho_f^\beta C^f T\mathbf{u}^f$, the heat transport equation can be obtained as

$$\left((1-\phi)\rho_s^s C^s T\right)^{\square} + \left(\phi\rho_f^f C^f T\right)^{\square} - \nabla\cdot\left(\lambda\nabla T\right) + \nabla\cdot C^f T\rho_f^f\mathbf{u} = \dot{Q} \tag{66}$$

where λ is the effective thermal conductivity of the porous media and can be estimated through $\lambda = (1-\phi)\lambda_s + \phi\lambda_f$, with λ_s, λ_f being the thermal conductivity coefficient of the solid and the fluid.

7 Numerical simulation for THMC-dissolution

This section presents the dissolution process in a coupled THMC framework through numerical simulation. It takes quartz dissolution in pure water solution as an example. The temperature influence on dissolution is first presented in a closed system scenario, which may be considered as dissolution taking place between an engineering facility and an aquitard. Later, the dissolution is modelled in an open system. The concentration change, dissolution rate and reaction extent are presented. The porosity and strain change due to dissolution in a long time scale are predicted.

7.1 Numerical model

The numerical model considers the dissolution of quartz in 2-dimentional rectangle with 0.5m width and 0.2m height. Quartz is the major mineral composition of clay /rock, and its

dissolution and corresponding influence is of significant interest to many research fields. The dissolution of quartz in water can be written as

$$SiO_2 + 2H_2O \rightarrow H_4SiO_4 \tag{67}$$

The dissolution rate equation is (Savage et al., 2002)

$$r = k_{rate} A_{sf} \left(1 - \left(\frac{Q}{K_{eq}} \right)^{\theta} \right)^{n} \tag{68}$$

in which r, k_{rate}, A_{sf} ,Q, K_{eq} are the dissolution rate in moles per unit volume porous media, rate constant, reactive surface area per unit volume of porous media, the ion activity product and the thermodynamic equilibrium constant, respectively. θ and n are two coefficients and set to be 1.

The dissolution rate constant k_{rate} is temperature-dependent, its simplified relationship with temperature is (Nguyen et al., 2016)

$$k_{rate} = k_{rate}^{25} \exp\left[-\frac{E_a}{R} \left(\frac{1}{T} - \frac{1}{298.15} \right) \right] \tag{69}$$

where k_{rate}^{25} is the rate constant at $25°C$, E_a is the activation energy, R is the gas constant.

The equilibrium constant K_{eq} is also temperature dependent. A lot of experiments have been done to investigate the solubility of quartz under different temperatures, pressure or pH (Morey et al., 1962; Fournier and Potter II, 1982; Manning, 1994; Rimstidt, 1997). Here, the empirical relationship proposed by Fournier is adopted as (Fournier and Potter II, 1982):

$$\log K_{eq} = -4.66206 + 0.0034063T + \frac{2179.7}{T} - \frac{1.1292\text{E}6}{T^2} + \frac{1.3543\text{E}8}{T^3} \tag{70}$$

The properties for quartz include molar mass: 60.086g/mol, molar volume: 22.68cm^3/mol surface area: 9.53E3m^2/m^3 (Guthrie and Carey, 2015), equilibrium constant: $1\text{E}-4$, $\log k_{rate}^{25} = 1\text{E}-16.3$ (Savage et al., 2002)

Other data adopted are listed in table 1

Table 1 parameters adopted for the simulation

Parameters	Physical meaning	Values and units

ϕ	porosity	0.2
K	Bulk modulus	1.875
C^s	Specific heat capacity of solid	835.5J/kg/K
C^w	Specific heat capacity of water	4202J/kg/K
λ_f	Thermal conductivity of fluid	1.5W/m/K
λ_s	Thermal conductivity of solid	1.23W/m/K

7.2 Numerical result

7.2.1 THMC-dissolution in closed system

1. Isothermal condition

Assume a closed system where there is no chemical exchange with the surroundings, but a chemical reaction takes place inside the system. The quartz will dissolve until equilibrium. Since the rate constant and equilibrium constant are temperature-dependent (Figure 1), the time it takes to reach equilibrium and the corresponding concentration must be different under different temperature, as shown in Figure 2. At 298.15K, from the adopted parameters, the dissolution will reach equilibrium at around 4 years with a H_4SiO_4 concentration of 1.18E-4mol/L. When the temperature rises to 350K, 380K and 400K, it takes 1000 hours, 200 hours, and 80 hours to reach equilibrium with H_4SiO_4 concentration of 5.00E-4 mol/L, 10.37E-4 mol/L and 16.14 E-4 mol/L.

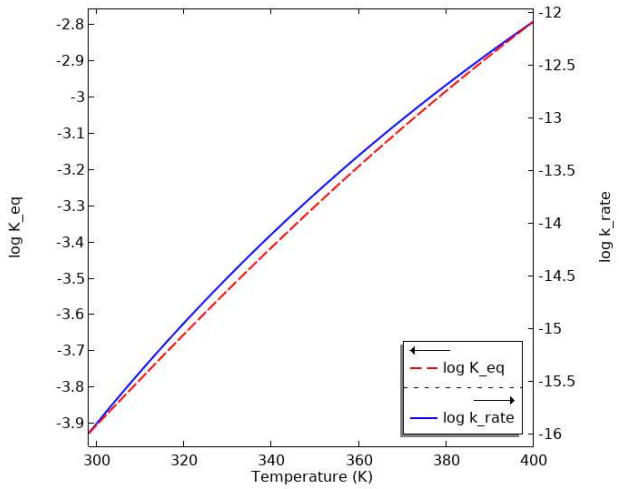

Figure 1 Equilibrium constant and rate constant change with temperature

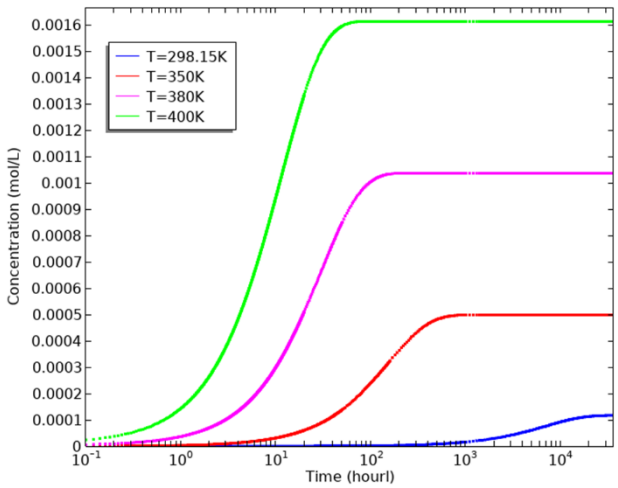

Figure 2 Concentration change with time under different temperature

2. Non-isothermal condition

The above section explored the temperature influence on the dissolution by assuming an isothermal condition. This section explores the chemical distribution in non-isothermal condition. To achieve this, a high temperature (T_left=350K or 400K) is applied on the left boundary and the domain is given a low temperature (298.15K). Due to the temperature gradient, heat will transfer from the left side to the right side gradually, resulting in time-dependent non-isothermal temperature distribution, as shown in Figure 3 and 5, the trend in the two situations are very similar.

Since the left side holds a higher temperature, the dissolution rate on the left side will be quicker than that on the right side, resulting in a high chemical concentration in the left domain. The concentration difference in the domain will further lead to a diffusion of chemicals from the left side toward the right side. Assuming a diffusion coefficient of 1.17E-9 (Rebreanu et al., 2008), the concentration distribution of H_4SiO_4 subject to dissolution and diffusion are presented in Figure 4 and 6, from which we could find that the concentration change at higher temperature is quicker.

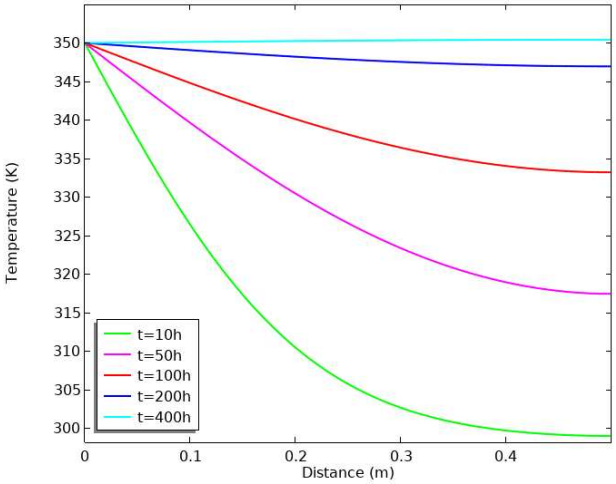

Figure 3 Temperature distribution with time and space (T_left=350K)

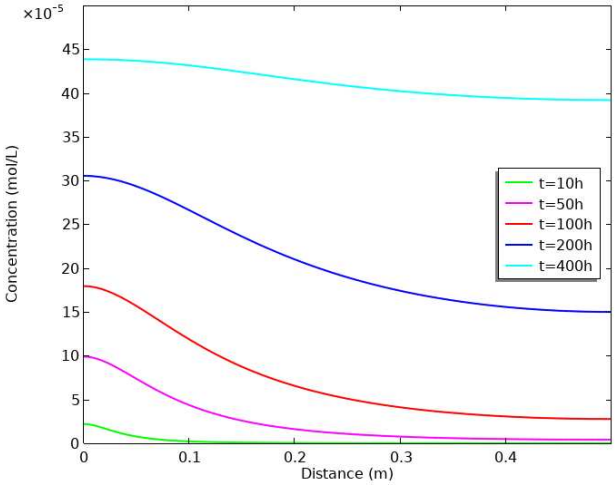

Figure 4 Concentration distribution with time and space (T_left=350K)

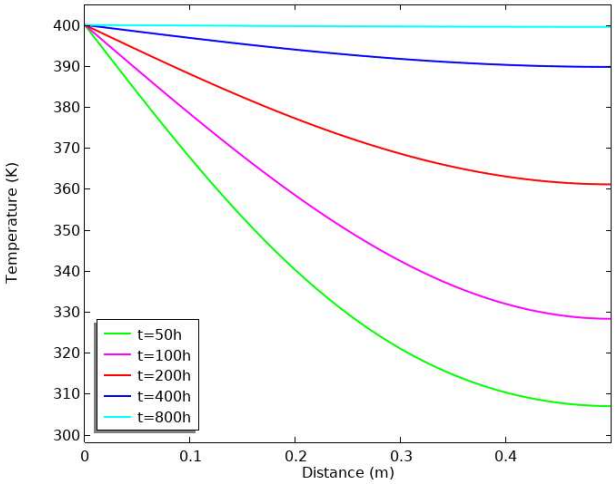

Figure 5 Temperature distribution with time and space (T_left=400K)

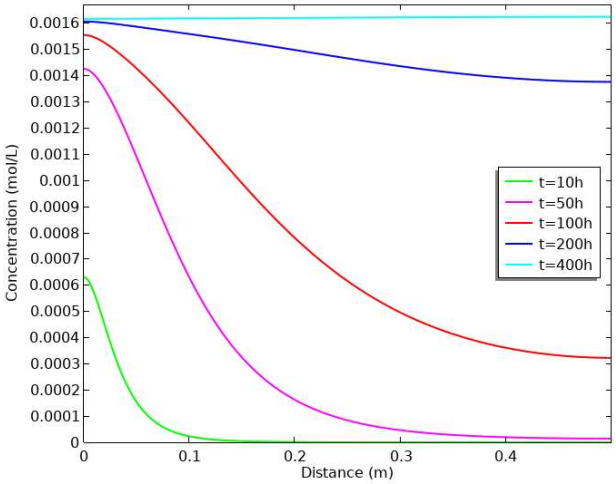

Figure 6 Concentration distribution with time and space (T_left=400K)

7.2.2 THMC-dissolution in open system

The above research investigated the temperature dependence of dissolution in a closed system, However, the dissolution process in a closed system, once reaching equilibrium, will no longer go further, which means that no more quartz can be further dissolved. Due to the very low solubility of quartz, the amount of quartz that can be dissolved is so limited that no significant influence on strain/porosity can be observed.

This section investigates the dissolution process in an open system. When reaching equilibrium, the concentration of dissolved species will no longer change, but the dissolution process keeps going, the chemicals generated from dissolution is the same as that been brought away by advection/diffusion, reaching a dynamic equilibrium status.

This time, it is assumed that the porous media is under a constant and uniform temperature of 350K. A fluid flow is injected into the media at a constant Darcy velocity of 1E-7m/s from the left toward the right. The concentration distribution will be controlled by advection, diffusion and reaction, as shown in Figure 7. It can be found that the concentration in the domain increase with time. After 400 hours, the concentration reaches a maximum value of 4.20E-4mol/L, which is less than the value in Figure 2. After 400 hours, the concentration does not change anymore, but the dissolution rate is nonzero (Figure 8), meaning that the dissolution process keeps going on. As given in equation (68), the dissolution is only associated with the concentration if assuming the reactive surface area to be constant, therefore, the trend in Figure 7 and 8 are very similar.

The incessant dissolution process will result in an increasing amount of reaction extent (Figure 9). At 10 years, the reaction extent is less than 0.1 moles per unit volume porous media while at 400 years, it reaches over 1.1 moles per unit volume porous media. Since the dissolution varies with space, the reaction extent also varies with space: the amount of quartz dissolved in the left domain is much more than that in the right domain, as shown in Figure 9.

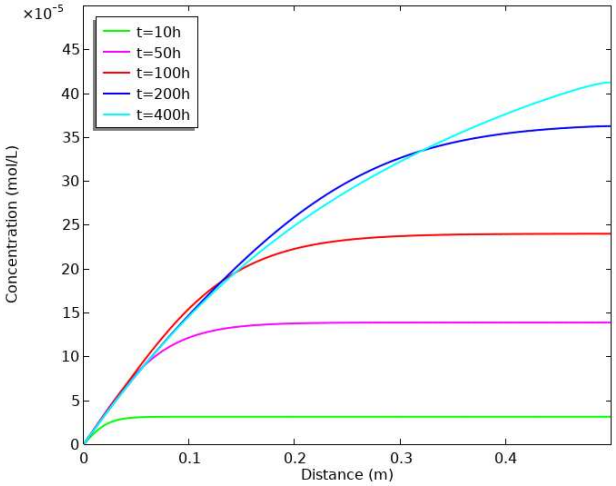

Figure 7 Concentration distribution with time and space (350K)

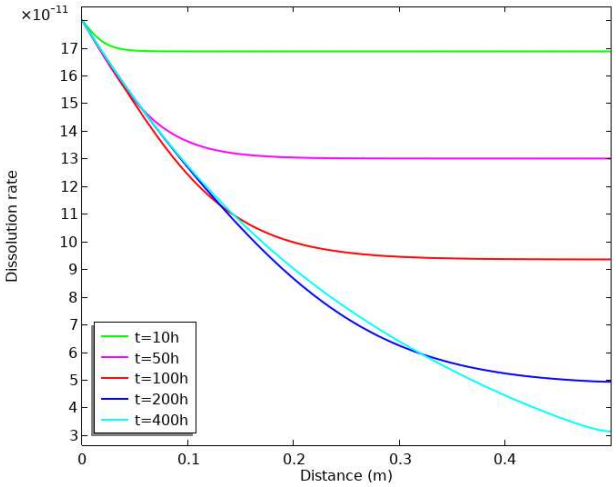

Figure 8 Dissolution rate distribution with time and space (350K)

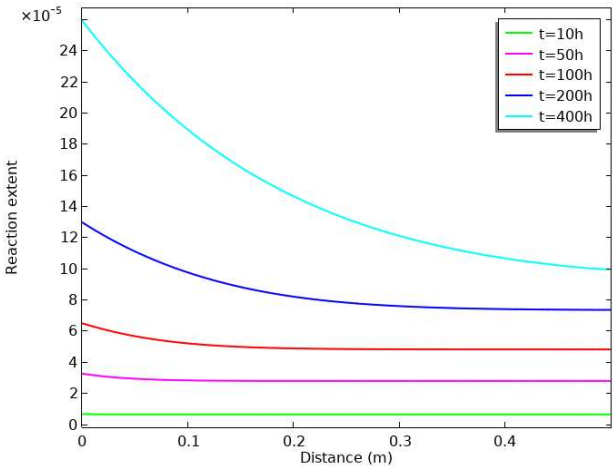

Figure 9 Reaction extent distribution with time and space (350K)

The porosity change is linked to the reaction extent through:

$$\Delta\phi = \frac{M^{qz}}{\rho_t^{qz}}\xi \tag{71}$$

where $\frac{M^{qz}}{\rho_t^{qz}} = 22.68cm^3/mol$ is the molar volume of quartz, $M^{qz} = 60.084g/mol$ is the molar mass of quartz and ρ_t^{qz} is the true density of quartz.

The strain resulting from dissolution is

$$\varepsilon_d = \frac{V_s^{rem}}{V_s^{ini}} - 1 = -\frac{M^{qz}}{\rho_t^{qz}}\frac{d(n)}{V_s} = -\frac{M^{qz}}{\rho_t^{qz}}\frac{1}{1-\phi}\xi \tag{72}$$

It can be found that the strain change and porosity change are both related to reaction extent and molar volume. The molar volume is so small and the reaction extent in Figure 9 is so tiny that within 400 hours, there could not be observable porosity/strain change. If the dissolution process takes place for a sufficiently long time, the amount of quartz that has been dissolved increases to a certain level, there could be a significant influence. As shown in Figure 10, when it comes to 10000 years, the porosity will increase by nearly 0.0013.

The porosity change can be more significant if the dissolution rate is quicker (temperature at 400K and Darcy velocity at 1E-6m/s), as seen in Figure 11. The corresponding strain resulting from dissolution can be easily estimated through relationship (72) and (71), and are presented in Figure 10 and 11 (strain is switched to positive to fit the strain definition in geotechnical engineering)

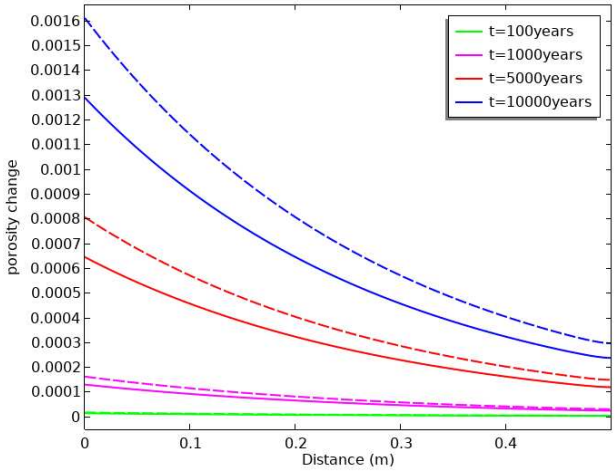

Figure 10 Porosity and strain change with time and space (350K) (Porosity: solid line, strain: dashed line)

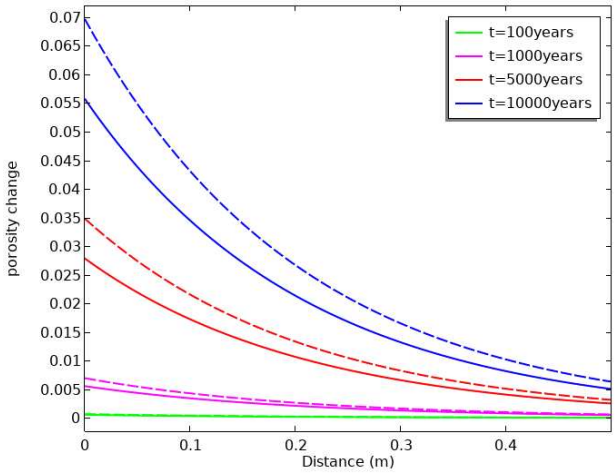

Figure 11 Porosity and strain change with time and space (400K) (Porosity: solid line, strain: dashed line)

8 Conclusion

In this paper, a novel non-equilibrium thermodynamics approach is proposed to derive the coupled Thermo-Hydro-Mechanical-Chemical formulation accounting for the complex reactive mineral dissolution. This approach quantifies the entropy production in a dissolution process with the knowledge from non-equilibrium thermodynamics and takes the Helmholtz free energy change as research object. A new concept, solid affinity, is introduced to describe the free energy change of the solid caused by dissolution. The approach overcomes the unclear description of reaction type and imprecise constitutive result of the Clausius-Duhem Inequality. The coupled Thermo-Hydro-Mechanical-Chemical equations with reactive dissolution are

derived by this approach. The role of dissolution is analysed and demonstrated through a simple numerical simulation.

The numerical results show that, in a closed system, the dissolution at a high temperature situation is much quicker than that in low-temperature condition and the equilibrium concentration is also higher under high temperature. In an open system, dissolution may reach a dynamics equilibrium status, in which case the dissolution keeps going on while the concentration remains constant. However, due to the sluggish dissolution rate, the amount of quartz that can be dissolved in a short time is very limited. If the dissolution keeps going on for over 100 years, the porosity change of strain can be significant.

CRediT authorship contribution statement

Yue MA: Conceptualization, Methodology, Software, Writing – original draft. **Shangqi GE:** Methodology, Writing – Original Draft. **He YANG:** Methodology, Writing – Original Draft **Xiaohui CHEN:** Conceptualization, Methodology, Supervision

Declaration of Competing Interest

The authors declare that they have no known competing financial interests or personal relationships that could have appeared to influence the work reported in this paper

Acknowledgements

The first author would like to thank the CERES studentship from the University of Leeds; The second and third authors would like to thank the financial support from the China Scholarship Council for their study at the University of Leeds.

Reference

Amanullah, M., Marsden, J., Shaw, H., 1994. Effects of rock-fluid interactions on the petrofabric and stress-strain behaviour of mudrocks, Rock Mechanics in Petroleum Engineering. OnePetro.

Bea, S.A., Mayer, U., MacQuarrie, K., 2016. Reactive transport and thermo‐hydro‐mechanical coupling in deep sedimentary basins affected by glaciation cycles: model development, verification, and illustrative example. Geofluids, 16(2): 279-300.

Chen, C., Zhang, L., Shen, P., 2020. Influence of mineral dissolution on the mechanical behaviour of a granular assembly under complex stress states. International Journal of Rock Mechanics and Mining Sciences, 136: 104546.

Chen, D., Yurtdas, I., Burlion, N., Shao, J.-F., 2007. Elastoplastic damage behavior of a mortar subjected to compression and desiccation. Journal of engineering mechanics, 133(4): 464-472.

Ciantia, M.O., Castellanza, R., Crosta, G.B., Hueckel, T., 2015. Effects of mineral suspension and dissolution on strength and compressibility of soft carbonate rocks. Engineering Geology, 184: 1-18.

Coussy, O., 1995. Mechanics of porous continua. Wiley.

Coussy, O., 2004. Poromechanics. John Wiley & Sons.

Fan, C., Luo, M., Li, S., Zhang, H., Yang, Z., Liu, Z., 2019. A thermo-hydro-mechanical-chemical coupling model and its application in acid fracturing enhanced coalbed methane recovery simulation. Energies, 12(4): 626.

Fournier, R.O., Potter II, R.W., 1982. An equation correlating the solubility of quartz in water from 25 to 900 C at pressures up to 10,000 bars. Geochimica et Cosmochimica Acta, 46(10): 1969-1973.

Gawin, D., Pesavento, F., Schrefler, B., 2003. Modelling of hygro-thermal behaviour of concrete at high temperature with thermo-chemical and mechanical material degradation. Computer Methods in Applied Mechanics and Engineering, 192(13-14): 1731-1771.

Gawin, D., Pesavento, F., Schrefler, B.A., 2008. Modeling of cementitious materials exposed to isothermal calcium leaching, considering process kinetics and advective water flow. Part 1: Theoretical model. Int J Solids Struct, 45(25-26): 6221-6240.

Gerard, B., Pijaudier-Cabot, G., Laborderie, C., 1998. Coupled diffusion-damage modelling and the implications on failure due to strain localisation. Int J Solids Struct, 35(31-32): 4107-4120.

Guimaraes, L.d.N., Gens, A., Sanchez, M., Olivella, S., 2006. THM and reactive transport analysis of expansive clay barrier in radioactive waste isolation. Communications in numerical methods in engineering, 22(8): 849-859.

Guthrie, G.D., Carey, J.W., 2015. A thermodynamic and kinetic model for paste–aggregate interactions and the alkali–silica reaction. Cem Concr Res, 76: 107-120.

Hasse.R, 1969. Thermodynamics of irreversible processes. Series in chemical engineering. Addison Wesley

Haxaire, A., Djeran-Maigre, I., 2009. Influence of dissolution on the mechanical behaviour of saturated deep argillaceous rocks. Engineering Geology, 109(3-4): 255-261.

Hosking, L.J., Chen, M., Thomas, H.R., 2020. Numerical analysis of dual porosity coupled thermo-hydro-mechanical behaviour during CO2 sequestration in coal. International Journal of Rock Mechanics and Mining Sciences, 135: 104473.

Hu, D., Zhou, H., Hu, Q., Shao, J., Feng, X., Xiao, H., 2012. A hydro-mechanical-chemical coupling model for geomaterial with both mechanical and chemical damages considered. Acta Mechanica Solida Sinica, 25(4): 361-376.

Jia, Y., Bian, H., Xie, S., Burlion, N., Shao, J., 2017. A numerical study of mechanical behavior of a cement paste under mechanical loading and chemical leaching. Int J Numer Anal Methods Geomech, 41(18): 1848-1869.

Karrech, A., 2013. Non-equilibrium thermodynamics for fully coupled thermal hydraulic mechanical chemical processes. Journal of the Mechanics and Physics of Solids, 61(3): 819-837.

Katchalsky, A., Curran, P.F., 1965. Nonequilibrium thermodynamics in biophysics. Harvard University Press, Cambridge, MA.

Kolditz, O., Shao, H., Wang, W., Bauer, S., 2016. Thermo-hydro-mechanical chemical processes in fractured porous media: modelling and benchmarking, 25. Springer.
Kondepudi, D., Prigogine, I., 2014. Modern thermodynamics: from heat engines to dissipative structures. John Wiley & Sons.
Kuhl, D., Bangert, F., Meschke, G., 2004. Coupled chemo-mechanical deterioration of cementitious materials. Part I: Modeling. Int J Solids Struct, 41(1): 15-40.
Lin, Y., Zhou, K., Li, J., Ke, B., Gao, R., 2020. Weakening laws of mechanical properties of sandstone under the effect of chemical corrosion. Rock mechanics and rock engineering, 53(4): 1857-1877.
Lyu, Q., Long, X., Ranjith, P., Tan, J., Kang, Y., Luo, W., 2018. A damage constitutive model for the effects of CO2-brine-rock interactions on the brittleness of a low-clay shale. Geofluids, 2018.
Ma, Y., Chen, X., Hosking, L.J., Yu, H.-S., Thomas, H.R., 2022. THMC constitutive model for membrane geomaterials based on Mixture Coupling Theory. Int J Eng Sci, 171: 103605.
Manning, C.E., 1994. The solubility of quartz in H2O in the lower crust and upper mantle. Geochimica et Cosmochimica Acta, 58(22): 4831-4839.
Momeni, A., Hashemi, S., Khanlari, G., Heidari, M., 2017. The effect of weathering on durability and deformability properties of granitoid rocks. Bulletin of Engineering Geology and the Environment, 76(3): 1037-1049.
Morey, G., Fournier, R., Rowe, J., 1962. The solubility of quartz in water in the temperature interval from 25 to 300 C. Geochimica et Cosmochimica Acta, 26(10): 1029-1043.
Nasir, O., Fall, M., Evgin, E., 2014. A simulator for modeling of porosity and permeability changes in near field sedimentary host rocks for nuclear waste under climate change influences. Tunnelling and Underground Space Technology, 42: 122-135.
Nguyen, B.N., Hou, Z., Bacon, D.H., Murray, C.J., White, M.D., 2016. Three-dimensional modeling of the reactive transport of CO2 and its impact on geomechanical properties of reservoir rocks and seals. International Journal of Greenhouse Gas Control, 46: 100-115.
Ning, L., Yunming, Z., Bo, S., Gunter, S., 2003. A chemical damage model of sandstone in acid solution. International journal of rock mechanics and mining sciences (1997), 40(2): 243-249.
Qi, S., Yue, Z.Q., Liu, C., Zhou, Y., 2009. Significance of outward dipping strata in argillaceous limestones in the area of the Three Gorges reservoir, China. Bulletin of Engineering Geology and the Environment, 68(2): 195-200.
Rebreanu, L., Vanderborght, J.-P., Chou, L., 2008. The diffusion coefficient of dissolved silica revisited. Marine chemistry, 112(3-4): 230-233.
Rimstidt, J.D., 1997. Quartz solubility at low temperatures. Geochimica et Cosmochimica Acta, 61(13): 2553-2558.
Savage, D., Noy, D., Mihara, M., 2002. Modelling the interaction of bentonite with hyperalkaline fluids. Applied Geochemistry, 17(3): 207-223.
Sun, L., Zhang, Y., Qin, Z., Wang, T., Zhang, S., 2020. A Damage Constitutive Model of Rock under Hydrochemical Cyclic Invasion. Advances in Civil Engineering, 2020.
Tao, J., Wu, Y., Elsworth, D., Li, P., Hao, Y., 2019. Coupled thermo-hydro-mechanical-chemical modeling of permeability evolution in a CO2-circulated geothermal reservoir. Geofluids, 2019.
Wriggers, P., 2008. Nonlinear finite element methods. Springer Science & Business Media.
Xiong, Y., Hu, L., Wu, Y.-S., 2013. Coupled geomechanical and reactive geochemical simulations for fluid and heat flow in enhanced geothermal reservoirs,

PROCEEDINGS, Thirty-Eighth Workshop on Geothermal Reservoir Engineering Stanford University.

Yin, S., Dusseault, M.B., Rothenburg, L.J.J.o.P.S., Engineering, 2011. Coupled THMC modeling of CO2 injection by finite element methods. 80(1): 53-60.

Zhang, R., Yin, X., Winterfeld, P.H., Wu, Y.-S., 2016. A fully coupled thermal-hydrological-mechanical-chemical model for CO 2 geological sequestration. Journal of Natural Gas Science and Engineering, 28: 280-304.

Zhang, X., Zhong, Z., 2017a. A coupled theory for chemically active and deformable solids with mass diffusion and heat conduction. Journal of the Mechanics and Physics of Solids, 107: 49-75.

Zhang, X., Zhong, Z., 2017b. A thermodynamic framework for thermo-chemo-elastic interactions in chemically active materials. SCIENCE CHINA Physics, Mechanics & Astronomy, 60(8): 084611.

Zhang, X., Zhong, Z., 2018. Thermo-chemo-elasticity considering solid state reaction and the displacement potential approach to quasi-static chemo-mechanical problems. International Journal of Applied Mechanics, 10(10): 1850112.

Zheng, L., Samper, J., Montenegro, L., Fernández, A.M., 2010. A coupled THMC model of a heating and hydration laboratory experiment in unsaturated compacted FEBEX bentonite. J Hydrol, 386(1): 80-94.